# Cambridge Centre for Computational Chemical Engineering


## University of Cambridge

Department of Chemical Engineering



Preprint ISSN 1473 – 4273


# Dual Injection HCCI Engine Simulation using a Stochastic Reactor Model


Sebastian Mosbach[1], Haiyun Su[1], Markus Kraft[1], Amit Bhave[2],

Fabian Mauss[3], Zhi Wang[4], Jian-Xin Wang[4]



submitted: December 9, 2005



[1] Department of Chemical Engineering
University of Cambridge, Pembroke Street
Cambridge CB2 3RA, UK
E-mail: sm453@cam.ac.uk
hs309@cam.ac.uk, mk306@cam.ac.uk

[2] Reaction Engineering Solutions Ltd.
61 Canterbury Street
Cambridge CB4 3QG, UK
E-mail: amitbhave@resolutionsltd.com

[3] Division of Combustion Physics
Lund Institute of Technology
Box 118, S-221 00 Lund, Sweden
E-mail: fabian.mauss@forbrf.lth.se

[4] Department of Automotive Engineering
Tsinghua University
Beijing 100084, China



Preprint No. 35


**c4e**


*Key words and phrases.* Homogeneous Charge Compression Ignition, dual injection, stochastic reactor models.

**Edited by**
Cambridge Centre for Computational Chemical Engineering
Department of Chemical Engineering
University of Cambridge
Cambridge CB2 3RA
United Kingdom.

**Fax:** + 44 (0)1223 334796
**E-Mail:** c4e@cheng.cam.ac.uk
**World Wide Web:** http://www.cheng.cam.ac.uk/c4e/

**Abstract**

Multiple direct injection (MDI) is a promising strategy to enable fast response ignition control as well as expansion of the homogeneous charge compression ignition (HCCI) engine operating window, thus realizing substantial reductions of soot and $NO_x$ emissions. In this work, we extend a probability density function based stochastic reactor model (SRM) for HCCI engines in order to incorporate MDI and an improved turbulent mixing model. For this, a simplistic spray model featuring injection, penetration, and evaporation sub-models is formulated, and mixing is described by the Euclidean minimal spanning tree (EMST) sub-model accounting for localness in composition space. The model is applied to simulate a gasoline HCCI engine, and the in-cylinder pressure predictions for single and dual injection cases show a satisfactory agreement with measurements. From the parametric studies carried out it is demonstrated that, as compared to single injection, the additional second injection contributes to prolonged heat release and consequently helps to prevent knock, thereby extending the operating range on the high load side. Tracking the trajectories of individual stochastic particles provides significant insight into the influence of local charge stratification due to direct injection on HCCI combustion.

# Contents

# 1 Introduction

Homogeneous charge compression ignition (HCCI) combustion, an advanced engine operation mode, is attracting significant attention from the combustion research community on account of its intrinsic benefits in terms of high efficiency and ultra-low emissions for $NO_x$ and soot, and due to the need to overcome technical obstacles such as difficulty in controlling ignition timing and a narrow operation range. Mixture formation in the combustion chamber using a fuel directly injected into compressed air (or air mixed with exhaust gas recirculation (EGR)) dictates the in-cylinder pressure, local temperatures, and local concentrations of the air-fuel-EGR mixture. Thus, direct fuel injection (DI) can influence the stratification of composition and temperature, and thereby control the auto-ignition timing and combustion duration. Individual single DI strategies such as early and late DI have been successfully used to demonstrate HCCI or HCCI-like combustion modes. However, single DI faces certain limitations, for instance, the problem with the soot-$NO_x$ trade-off persists with single late DI or high injection pressures for Diesel fuel, whereas late direct injection with gasoline can result in knock [1, 2]. Multiple direct injection (MDI) strategy has the potential for a robust, fast response in ignition timing control and also for expanding the HCCI operating window over the load-speed sweep [1].

Experimental research involving MDI schemes for a range of conventional as well as alternative fuels has been widely reported. In recent years, optical experimental studies of MDI strategies of Diesel and other synthetic fuels have been carried out, with the number of injection pulses as high as 5 or 9 within an engine cycle. Merits of MDI in terms of improving the homogeneity of the in-cylinder mixture, increasing the combustion efficiency, and lowering soot concentrations have been observed [3, 4, 5]. Another study involving two-stage injection in a partially premixed charge compression ignition (PCCI) engine demonstrated the role of reduced wall-wetting, higher peak heat release rate after first injection, and better evaporation even early in the compression stroke on improvements in thermal efficiency and lowering of $NO_x$ and soot emissions [6]. A second injection has been used as an ignition-trigger and control mechanism in a diesel fuelled DI HCCI engine. For optimized conditions, sufficient torque was generated under low $NO_x$ and soot emissions [7].

In case of gasoline fuelled engines, a dual-injection strategy has been proposed, in which a homogeneous lean air-fuel mixture (from first early DI during intake stroke) compressed close to conditions favourable for HCCI combustion, was ignited using the second stage injection (stratified charge) [2]. This strategy is further assisted with spark discharge by reducing the cyclic fluctuations in combustion [8, 9]. Utilizing the thermal energy of the hot trapped EGR combined with dual injection in a 6-S gasoline direct injection (GDI) engine has been introduced [10]. Another MDI strategy comprising of injecting a portion of fuel into the trapped internal EGR during negative valve overlap and injecting the remaining fuel in the intake stroke has also been proposed. The first stage injection enabled fuel reforming and improving the ignitability of the fuel, and this dual injection scheme expanded the lean limit of HCCI combustion without increase in $NO_x$ emissions [11]. Optimizing

a set of injection parameters and intake temperature to obtain significant reduction in fuel consumption and emissions for a dual injection HCCI engine has also been reported [12].

Compared to experimental MDI HCCI studies, computational modelling investigations have been limited. In general, for simulating single early DI HCCI combustion, a range of tools such as single-zone, multi-zone and probability density function (PDF) based engine cycle simulators as well as 3D CFD models have been implemented [13, 14, 15, 16, 17]. However, for MDI operation, only studies involving CFD models have been reported. A dual-stage DI HCCI operation has been simulated using a 3D CFD code containing a hollow cone spray sub-model and a combustion model based on the Shell auto-ignition reaction and eddy dissipation concept (mean reaction rate), resulting in computational time of the order of 7 days on an SGI machine (400 MHz) [18]. In a brief study elsewhere, the influence of dual injection on in-cylinder pressure in a Diesel fuelled PCCI engine has been validated against experiments [19]. Recently, the role of multi-pulse injections in controlling premixed mixture preparation was modelled during the closed volume part of the cycle in a dodecane fuelled engine, using a commercial 3D CFD code [20]. For an earlier DI timing, the pulse width showed a strong impact on evaporation and mixing, whereas for late DI, a short dwell time was influential in uniform fuel stratification. However, the influence of combustion in evaluating the mixing process was not accounted for. Inclusion of a detailed description of chemical kinetics – vital for HCCI combustion – within the CFD model framework would put an additional demand on the computational power. This expense can be significantly reduced using integrated engine cycle models while maintaining the reduced predictive power within an acceptable range. The single- and multi-zone based full cycle simulators have only been implemented for early DI HCCI simulations.

In this paper, we present a PDF based stochastic reactor modelling (SRM) approach to account for MDI which can be easily incorporated in an engine cycle code without major modifications. The SRM approach with its inherent benefits in terms of detailed kinetics description and ability to account for inhomogeneities as demonstrated in our previous work for single early DI [14] and port fuel injected HCCI combustion [21] is extended by formulating and incorporating a simplistic spray model and an improved turbulent mixing model.

This paper is structured as follows. In the next section, the numerical model is presented and the spray sub-model and its implementation in the SRM framework is explained. In the following section, we present results of numerical simulations in which the model is applied to simulate a dual injection HCCI engine and is validated against measurements. A discussion on stratification in composition space, and parametric investigations related to DI are included. Finally, we draw some conclusions and identify open questions for future work and development.

# 2 Extension of the SRM to direct injection including spray

## 2.1 Summary of the stochastic reactor model

We briefly recall some fundamentals of the SRM successfully employed earlier [21] in order to describe in the next subsection the inclusion of the direct injection and spray model. Due to space limitations, we do not repeat here the main model equation, namely the PDF transport equation [22]. The output of the model consists of (distributions of) the species mass fractions $Y_j$ and temperature $T$, combined into a vector $\psi = (Y_1, \ldots, Y_S, T)$ for notational convenience, where $S$ denotes the number of chemical species. The source terms generating the time evolution of the PDF represent the various physical processes taken into account by the model, i.e. chemical kinetics, turbulent mixing, piston movement, and convective heat transfer. The chemical reactions and their heat release including temperature change due to compression and expansion are summarized in the function $G$ defined by

$$\begin{aligned} G_j(\psi) &= \frac{M_j \dot{\omega}_j}{\varrho}, \qquad j = 1, \ldots, S \\ G_{S+1}(\psi) &= -\frac{1}{c_V \varrho} \sum_{i=1}^{S+1} e_i M_i \dot{\omega}_i - \frac{p}{c_V m} \frac{\mathrm{d}V}{\mathrm{d}t}, \end{aligned} \tag{2.1}$$

which generates the time evolution of the mass fractions and the temperature. Here, $M_j$ denotes the molar mass, $\dot{\omega}_j$ the molar production rate, and $e_i$ the specific internal energy of the $j^{\text{th}}$ species. $\varrho$ denotes the mass density, $c_V$ the specific heat capacity at constant volume, $m$ the total mass, and $V$ the instantaneous cylinder volume. This function $G$ will be modified in the following subsection to incorporate a simplistic spray model.

For the description of turbulent mixing we use the Euclidian Minimal Spanning Tree (EMST) model [23]. We elaborate in detail on the role of mixing below.

## 2.2 Spray model

The spray model we employ consists of three parts, namely an injection, a penetration, and an evaporation sub-model. The shape of the spray (the droplet cloud) remains unspecified, i.e. we do not take into account geometrical information such as the spray tip penetration or the cone angle. However, under certain assumptions these quantities could be related to one of the parameters used in our model.

Concerning injection we assume that the population of droplets entering the cylinder possesses a user-specified Sauter mean diameter (SMD). Recall that the SMD is defined such that a fictitious population of identical droplets each with a diameter equal to SMD possesses the same total volume and surface area as the actual

population considered. Since the surface area of the droplets is the relevant quantity as far as evaporation is concerned, one can safely assume for this purpose that the droplet diameter of every droplet equals SMD. For Diesel fuels, an empirical expression has been proposed [24, 25] and used to develop a zero dimensional spray model [26]. Similar work for gasoline has not yet been carried out to the knowledge of the authors.

In the penetration sub-model we assume that the inflowing fuel is distributed at a constant rate such that no fluid parcel receives fuel at more than one instant in time. More quantitatively, in a time step $\Delta t$, the mass of cylinder charge that is to be endowed with fuel droplets is given by $\alpha\Delta t$, where $\alpha$ is a model parameter. Physically, larger $\alpha$ corresponds to more evenly spread fuel, i.e. greater cone angle or tip penetration. Contrariwise, smaller $\alpha$ implies stronger charge stratification.

The mass flow rate for the evaporation of a single droplet can be calculated from elementary considerations [27] (mass conservation). In our case this leads to an equation describing the time evolution of the liquid fuel mass of the entire population

$$\dot{m}_{\mathrm{liq}} = -\frac{3}{2}\lambda_{\mathrm{evap}}\left(\frac{\pi}{6}\varrho_{\mathrm{liq}}N_{\mathrm{d}}\right)^{2/3} m_{\mathrm{liq}}^{1/3},$$

where $\lambda_{\mathrm{evap}}$ is an evaporation constant, $\varrho_{\mathrm{liq}}$ is the mass density of the liquid fuel, and $N_{\mathrm{d}}$ is the number of droplets in the population. The solution of this equation is given by

$$m_{\mathrm{liq}}(t) = \left[m_{\mathrm{liq}}(t_0)^{2/3} - \left(\frac{\pi}{6}\varrho_{\mathrm{liq}}N_{\mathrm{d}}\right)^{2/3}\lambda_{\mathrm{evap}}(t-t_0)\right]^{3/2}. \tag{2.2}$$

Note that this implies that the evaporation time (the time it takes for a droplet to evaporate) is given by $\tau_{\mathrm{evap}} = \mathrm{SMD}^2/\lambda_{\mathrm{evap}}$. A physical interpretation of $\lambda_{\mathrm{evap}}$ is the change of surface area of a single droplet per unit time.

The PDF transport equation is extended to include this model simply by appending the scalar $m_{\mathrm{liq}}$ to $\psi$, i.e. $\psi = (Y_1, \ldots, Y_S, T, m_{\mathrm{liq}})$. The time evolution of $m_{\mathrm{liq}}$ is then described by

$$G_{S+2}(\psi) = -\frac{3}{2}\lambda_{\mathrm{evap}}\left(\frac{\pi}{6}\varrho_{\mathrm{liq}}N_{\mathrm{d}}\right)^{2/3}\psi_{S+2}^{1/3}. \tag{2.3}$$

Apart from that, the equation for the SRM remains unaltered.

# 3 Extension of the algorithm

The extended SRM (the PDF transport equation together with (2.3)) is solved as previously [21] by an operator splitting technique combined with a Monte Carlo method, in which the PDF is approximated by a notional ensemble of $N_{\mathrm{par}}$ stochastic particles. Now, however, each particle carries $S+2$ scalars, namely not only the mass fractions and temperature, but also the liquid fuel mass, i.e. $\psi^{(i)} = (Y_1^{(i)}, \ldots, Y_S^{(i)}, T^{(i)}, m_{\mathrm{liq}}^{(i)})$. All $m_{\mathrm{liq}}^{(i)}$ are initialized with zero, and the mass fractions are

normalized as usual, i.e. $\sum_j Y_j^{(i)} = 1$. For convenience, the number of droplets $N_\mathrm{d}^{(i)}$ is also associated to each particle for the purpose of implementation, but this is not an additional scalar and hence neither appears explicitly in $\psi$ nor in the PDF transport equation.

Since in the present work there is no in-/outflow of stochastic particles, and the injection by construction does not affect the particle number at all, there is no need for down-sampling (reduction of the number of particles whilst conserving the PDF as well as possible), in contrast to [14]. However, this becomes necessary again as soon as the method considered here is incorporated into a full cycle simulation, which is easily achieved.

The following model parameters are required as input: the mass density $\varrho_\mathrm{liq}$ of the liquid fuel, the mass flow rate $\dot{m}_\mathrm{fuel}$ of the injected fuel, the SMD, the evaporation constant $\lambda_\mathrm{evap}$, and the constant $\alpha$ measuring the spray penetration. The mass flow rate $\dot{m}_\mathrm{fuel}$ is also assumed constant during the injection process. Note that the constant parameters SMD, $\lambda_\mathrm{evap}$, and $\alpha$ can be replaced by sub-models calculating them based on physical properties of the fuel and geometrical information of the injector, thereby leaving room for future developments and improvements.

The only modification made to the SRM source code is one additional splitting step which accounts for combined injection and penetration and one for evaporation. If the current crank angle lies between $\mathrm{SOI}_2$ and $\mathrm{EOI}_2$ then the following **splitting step for injection and penetration** is performed.

1. Pick particles randomly according to statistical weight such that the sum of the masses of the particles does not exceed $\alpha\Delta t$ and that no particle which has been chosen previously is picked again. Assign to each of the chosen particles a value of $m_\mathrm{liq}^{(i)}$ proportional to the statistical weight such that the total injected mass $\sum m_\mathrm{liq}^{(i)}$ per time step $\Delta t$ equals $\dot{m}_\mathrm{fuel}\Delta t$, i.e.

$$m_\mathrm{liq}^{(i)} = \frac{W^{(i)}}{\sum W^{(j)}} \dot{m}_\mathrm{fuel}\Delta t,$$

   where the sum ranges over the indices of the chosen particles.

2. Calculate the droplet numbers according to

$$N_\mathrm{d}^{(i)} = \frac{6m_\mathrm{liq}^{(i)}}{\pi\varrho_\mathrm{liq}\mathrm{SMD}^3} \qquad \forall i \in \{1,\ldots,N_\mathrm{par}\}.$$

After the second injection has started, if there is still liquid fuel left, then the following **splitting step for evaporation** is performed.

1. Update the liquid fuel mass of all particles, i.e. for each $i \in \{1,\ldots,N_\mathrm{par}\}$ set $m_\mathrm{liq}^{(i)} \mapsto \tilde{m}_\mathrm{liq}^{(i)}$, where

$$\tilde{m}_\mathrm{liq}^{(i)} = \left[(m_\mathrm{liq}^{(i)})^{2/3} - \left(\frac{\pi}{6}\varrho_\mathrm{liq}N_\mathrm{d}^{(i)}\right)^{2/3}\lambda\Delta t\right]^{3/2}$$

or set $m_{\mathrm{liq}}^{(i)}$ (and $N_{\mathrm{d}}^{(i)}$) to zero if the expression in square brackets is non-positive.

2. Update the statistical weights according to

$$W^{(i)} \mapsto W^{(i)} + m_{\mathrm{liq}}^{(i)} - \tilde{m}_{\mathrm{liq}}^{(i)} =: \tilde{W}^{(i)}$$

for all $i \in \{1, \ldots, N_{\mathrm{par}}\}$.

3. Update the (gaseous) species mass fractions according to

$$Y_j^{(i)} \mapsto Y_j^{(i)} \frac{W^{(i)}}{\tilde{W}^{(i)}} =: \tilde{Y}_j^{(i)} \quad \forall j \neq \text{fuel}$$

$$Y_{\mathrm{fuel}}^{(i)} \mapsto 1 - \sum_{j=1, j\neq\mathrm{fuel}}^{S} \tilde{Y}_j^{(i)}$$

for all $i \in \{1, \ldots, N_{\mathrm{par}}\}$, where 'fuel' denotes the indices of all fuel species.

# 4 Numerical study

## 4.1 Model calibration

**Table 1:** *Engine specification and operating condition.*

| | |
|---|---|
| Bore×Stroke | $95 \times 115$ mm$^2$ |
| Displaced volume | 815 cm$^3$ |
| Connecting rod length | 210 mm |
| Compression ratio (CR) | 11 |
| Speed | 1400 RPM |
| Air/fuel equiv. ratio | 1.6 |
| EGR (internal+external) | 20% |
| Inlet valve opening (IVO) | 350 CAD ATDC |
| Inlet valve closing (IVC) | 150 CAD BTDC |
| Exh. valve opening (EVO) | 120 CAD ATDC |
| Exh. valve closing (EVC) | 370 CAD ATDC |
| Start of 1$^{\mathrm{st}}$ inj. ($\mathrm{SOI}_1$) | 340 CAD BTDC |
| Start of 2$^{\mathrm{nd}}$ inj. ($\mathrm{SOI}_2$) | 40 CAD BTDC |

The implementation of the model was built upon a version used in previous work [21]. The new sub-models discussed in the previous section were integrated into this existing code. All simulations were carried out on AMD Athlon 3000+ Linux PCs running at 2.16 GHz.

For the calibration and validation of our model we use experimental data obtained previously [9]. The experiments were carried out on a 2 cylinder in-line 4 stroke direct injection gasoline engine which was naturally aspirated. Main engine and operating parameters are listed in Table 1. We model the fuel as being composed of iso-octane (mass fraction 0.859) and n-heptane (mass fraction 0.141), which corresponds to an octane number of 88 (experiment: RON= 90.6, MON= 81). The chemical mechanism describing the kinetics contains 157 species and 1552 reversible reactions.

Since in this study we focus mainly on the second (i.e. late) injection, we restrict our simulations to the closed-volume part of cycle (i.e. from IVC to EVO), so for the time being we neglect the gas exchange during the engine breathing process. The start of the first injection $\mathrm{SOI}_1$ is timed shortly after IVO close to top dead center (see Table 1). As a consequence of the rapid turbulent mixing during the intake process, we assume as initial condition at IVC that the cylinder charge is homogeneous in temperature as well as in composition.

A central feature of direct injection is the charge stratification it gives rise to, which underlines the importance of accurate modelling of the turbulent mixing process. The simplest mixing model is the Interaction by Exchange with the Mean (IEM) model, in which all scalars relax exponentially to their mean value. One (out of several) unphysical aspects of this model is that every particle can mix with any other particle in phase space. Using IEM in our simulations results in too rapid dilution of the injected fuel, even for slow mixing (i.e. large turbulent mixing times $\tau$). Much more suitable for out purposes is the EMST model [23], in which particles to be mixed are chosen based on proximity in phase space.

As for the choice of the turbulent mixing time $\tau$, we find that in order to reproduce experimental measurements, intensified mixing (i.e. a shorter mixing time) is necessary during the injection period. Reduced mixing times during injection have been observed previously in CFD simulations (see for example Fig. 7 in [15]). In all our simulations we used $\tau = 0.5$ ms during injection and $\tau = 4$ ms otherwise, values which are very similar to those found in [15]. The mixing time parameter determines how long any charge stratification is maintained, or in other words how quickly locally rich conditions are diluted. Too rapid mixing would result in a relatively homogeneous charge at the time of ignition, similar to a single early injection or even port injection.

For all dual injection simulations we used as in the experiments a split ratio of $6:1$ (ratio of fuel masses injected into the cylinder during the first and second injection). With a total injected fuel mass of 21.6 mg, the fuel injected during second injection constitutes of order 0.1% of the total mass inside the cylinder. Therefore, we made the simplifying assumption that the temperature of the charge is not affected by the second injection.

The SMD has been chosen as follows. The fuel injector used in the experiments was designed to produce droplet distributions with SMD= 15 $\mu$m for injection into atmospheric ambient pressure. However, at the conditions of late injection ($-40$ CAD)

the ambient in-cylinder pressure is much larger (about 7 bar), which tends to lead to significantly bigger droplets [25]. Typical values for Diesel fuel lie roughly in the range between 25 and 75 $\mu$m [25], but for gasoline smaller values are expected [28] partly due to the lower viscosity, which is consistent with the design specification of the employed injector. Based on these considerations, we somewhat arbitrarily chose SMD= 27 $\mu$m throughout. Reasonable estimates for $\lambda_{\text{evap}}$ yield values of order 1 mm$^2$/s which for an SMD of 27 $\mu$m corresponds to an evaporation time of $\tau_{\text{evap}} \approx 0.73$ ms (or 6.1 CAD at 1400 RPM).

Before the model can be applied to investigative studies, several model parameters need to be calibrated. Some results of this tuning process are shown in Fig. 1. For the dual injection case we used an evaporation constant of $\lambda_{\text{evap}} = 0.6$ mm$^2$/s and $\alpha = 20$. The number of stochastic particles was chosen $N_{\text{par}} = 100$ unless indicated otherwise.

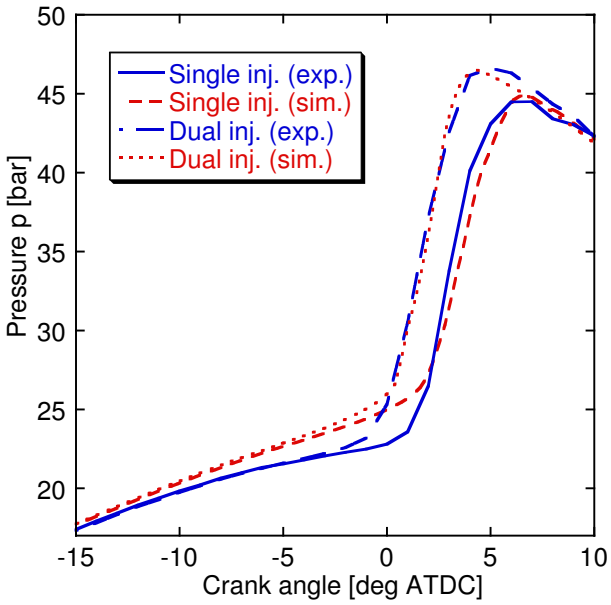


**Figure 1:** *Experimental and simulated in-cylinder pressure profiles for single and dual injection.*

Under these particular conditions, the dual injection is seen to have very little effect on the shape of the pressure profile, experimentally as well as numerically. The difference in ignition timing is found to be due to different temperatures at IVC (by about 4 K). The remainder of this paper focusses on exhibiting under which circumstances the pressure profiles are affected by a second injection and how.

## 4.2 Results and discussion

Figure 2 depicts the time evolution of the total in-cylinder liquid fuel mass for various values of the evaporation constant $\lambda_{\text{evap}}$. Recall that large values of $\lambda_{\text{evap}}$ correspond

to short evaporation times (via $\tau_{\text{evap}} = \text{SMD}^2/\lambda_{\text{evap}}$). The start (at $-40$ CAD) and the end (at $-37$ CAD) of the second injection are readily discernible, as are the different evaporation time scales.

Figure 3 displays the average mass fraction of gaseous iso-octane in the cylinder as function of the crank angle for $\alpha = 20$. Until $\text{SOI}_2 = -40$ CAD the iso-octane mass fraction stays constant because fuel consumption (pyrolysis, thermal decomposition, OH radical attack) has not yet set in. After the second injection has begun, the mass of iso-octane rises as expected. Again, one can clearly see the effect of different $\lambda_{\text{evap}}$. Roughly at the same time the gaseous fuel starts to be consumed. We also looked at the consumption of iso-octane for different levels of stratification, i.e. different values of $\alpha$. It was consumed more rapidly for stronger stratification (smaller $\alpha$), though this effect was small.

In Figs. 4, 5, and 6 we illustrate the effect of varying the spray model parameters $\alpha$ and $\lambda_{\text{evap}}$ on the pressure profile. Figure 4 demonstrates the influence of varying the level of charge stratification, i.e. choosing different values of $\alpha$. For all the curves $\lambda_{\text{evap}} = 1.2$ mm$^2$/s (short evaporation time). For the case of medium evaporation time the curves turn out very similar to those shown, but for long evaporation time all curves basically coincide with each other, which means that the effect of charge stratification is no longer visible. A possible explanation for this is that in the latter case too little fuel is released into the gas phase per unit time, so that there is enough time to dilute it. In particular, the mixture might be overall too dilute so that the stratification has virtually no influence. For $\alpha = 20$, the case of strongest stratification, the combustion duration is prolonged compared to the other cases by more than 2 CAD, and the pressure profile agrees much better with the experimental one.

Figure 5 shows again the influence of the stratification level for medium evaporation constant $\lambda_{\text{evap}} = 0.6$ mm$^2$/s and higher resolution, which corroborates the trend exhibited in Fig. 4, namely the higher the level of stratification the longer the combustion duration. The number of stochastic particles determines the resolution of the model, i.e. the maximum attainable stratification: For a given particle number $N_{\text{par}}$, the maximal stratification which can be resolved by the model is reached if precisely one particle receives liquid fuel per time step. For example, at $N_{\text{par}} = 100$ this limit of resolution is attained for $\alpha = 20$ roughly. Higher levels of stratification, i.e. smaller values of $\alpha$, can be reached for larger $N_{\text{par}}$. In Fig. 5, for each $N_{\text{par}}$, $\alpha$ has been chosen such that only one particle receives fuel per time step. Note that one cannot pick a fixed number of particles to be endowed with liquid fuel, because then predictions of the model would depend on the numerical parameter $N_{\text{par}}$. This is a main reason for introducing $\alpha$, a physical parameter, because the stratification is then independent of $N_{\text{par}}$ (at least asymptotically for large particle numbers). The simulation for $N_{\text{par}} = 100$, $\alpha = 20$ required a CPU-time of 50 minutes, which is also the typical CPU-time for most of the other runs performed in this work. The run for $N_{\text{par}} = 200$, $\alpha = 10$ took 1h 50min, and the one for $N_{\text{par}} = 500$, $\alpha = 4$ required 5h 30min of computation.

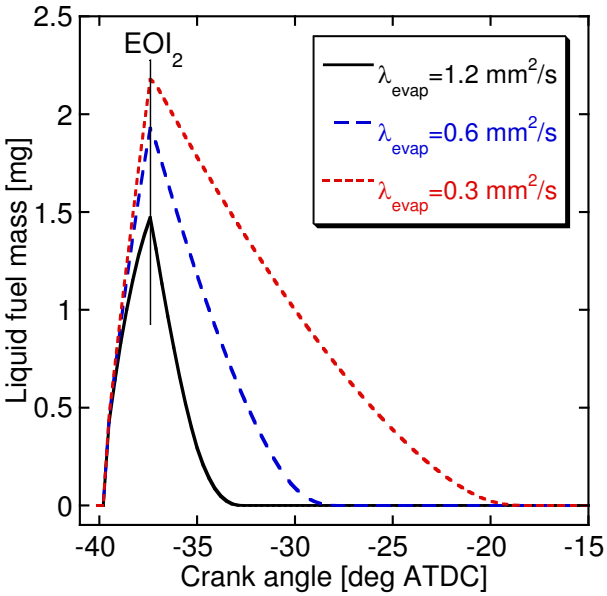


**Figure 2:** *Time evolution of the total in-cylinder liquid fuel mass for various values of the evaporation constant $\lambda_{evap}$ (start of second injection $SOI_2 = -40$ CAD, end of second injection $EOI_2 = -37.4$ CAD).*

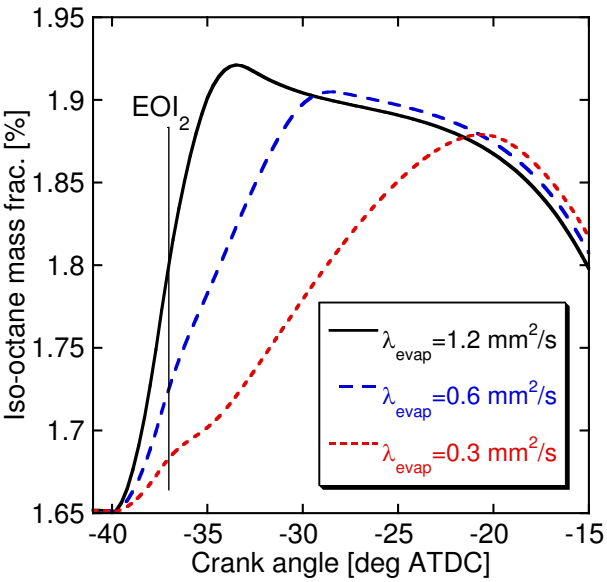


**Figure 3:** *Time evolution of the average mass fraction of (gaseous) iso-octane for various values of the evaporation constant $\lambda_{evap}$ at $\alpha = 20$ (start of second injection $SOI_2 = -40$ CAD, end of second injection $EOI_2 = -37.4$ CAD).*

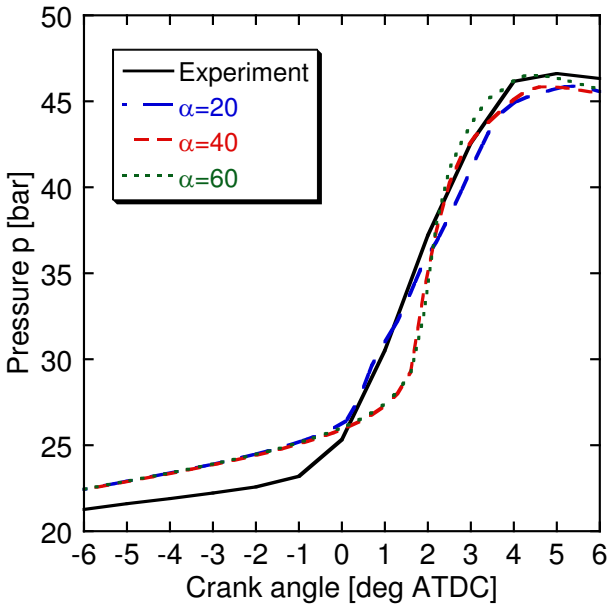


**Figure 4:** *Pressure profiles for various levels of charge stratification at* $\lambda_{evap} = 1.2\ mm^2/s$ *(short evaporation time) compared to experiment.*

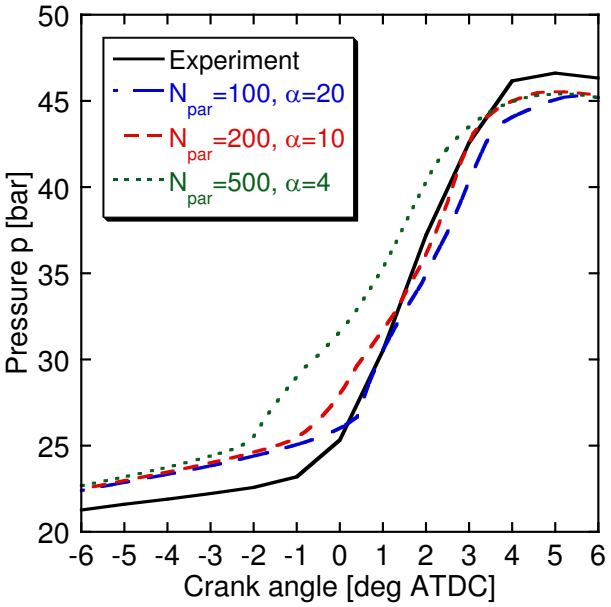


**Figure 5:** *Pressure profiles for various levels of charge stratification at higher resolution and* $\lambda_{evap} = 0.6\ mm^2/s$ *compared to experiment.*

Figure 6 illustrates the impact of varying $\lambda_{\text{evap}}$ on the pressure profile for maximum stratification ($\alpha = 20$). We recognize that shorter evaporation times promote stratification and therefore the spreading of heat release, consistently with the previous two figures. For lower stratification levels (greater $\alpha$), all considered pressure profiles exhibit large pressure rise rates at ignition (short combustion duration) with virtually no dependence on the evaporation time.

Figure 7 gives some insight into the local evolution of temperature and gaseous iso-octane mass fraction of fluid parcels inside the cylinder. The curves labelled 'fuel' belong to a single stochastic particle which receives liquid fuel during the second injection, whereas the curves referred to as 'lean' belong to a particle which does not. The cylinder average is labelled 'mean'. The effects of evaporation (until about -30 CAD ATDC) and the chemical kinetics of the gaseous iso-octane (until TDC) of the fuel particle demonstrate a faster depletion of iso-octane compared to that for the lean particle and the mean iso-octane level. The fuel particle ignites about 3 CAD earlier than the lean one and its local peak temperature exceeds the average by almost 500 K.

Finally, we note that none of the observations made are sensitive towards the timing of the second injection.

# 5 Conclusions

Dual injection in a gasoline HCCI engine is studied using a PDF based stochastic reactor modelling approach. The model includes detailed kinetics and accounts for inhomogeneities in composition and temperature on account of turbulent mixing, convective heat transfer and direct injection. A simplistic spray model describing injection, penetration, and evaporation sub-processes is developed. For mixing the EMST model which accounts for localness in composition space is employed.

The predicted ignition timing and the peak pressure agreed satisfactorily with measurements, for both single and dual-injection cases. Systematic parametric studies related to spray penetration and characteristic evaporation lag demonstrate the role of increased charge stratification induced by direct injection in prolonging the combustion duration and increasing the rate of iso-octane consumption. Furthermore, it was shown that raising the number of stochastic particles improved the maximum attainable stratification in the model, but also increased the computational expense.

Tracing individual stochastic particles revealed that the particles receiving fresh fuel from the second injection experienced advanced auto-ignition compared to the lean particles not exposed to fresh fuel. This observation further substantiated the role of dual injection in widening the heat release, thereby increasing the HCCI operating limit to higher loads.

With the focus of the present work on gaining insight into the influence of dual injection on combustion parameters on local and global levels; improving the spray sub-model, full cycle simulations and a detailed study of the influence of multiple

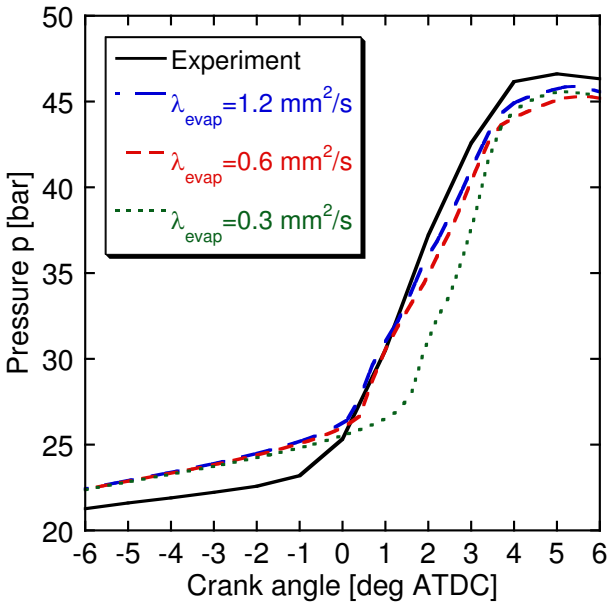


**Figure 6:** *Pressure profiles for various evaporation constants at $\alpha = 20$ compared to experiment.*

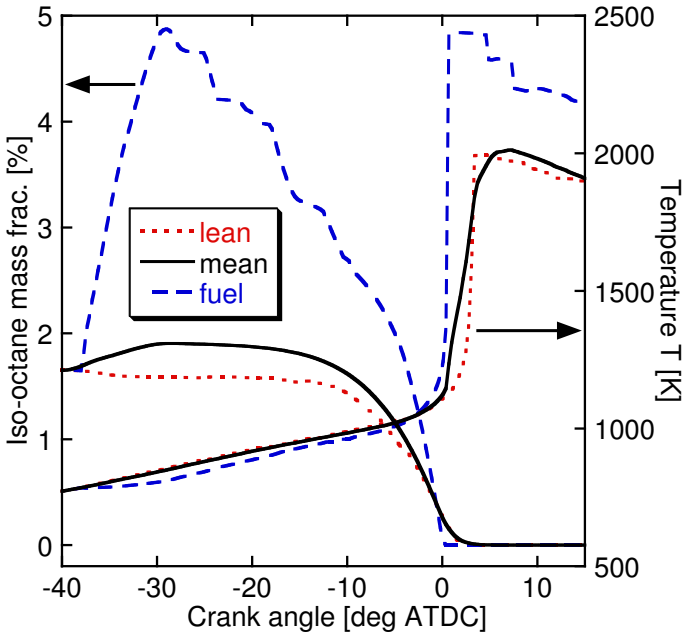


**Figure 7:** *Local history of temperature and iso-octane mass fraction, for single particles ('fuel' and 'lean') and in-cylinder average ('mean').*

injections on emissions form the scope of future work.

**Acknowledgments**

This work was partially funded by the EPSRC (grant number GR/R85662/01).

# References

[1] F. Zhao. HCCI control and operating range extension. In *Homogeneous Charge Compression Ignition (HCCI) Engines: Key Research & Development Issues*, SAE Publication PT-94, pages 325–348, March 2003.

[2] C. D. Marriott and R. D. Reitz. Experimental investigation of direct injection gasoline for premixed compression-ignited combustion-phasing control. SAE Paper No. 2002-01-0418, 2002.

[3] T. Delebinski, P. Eckert, and G. P. Merker. Optical investigation of HCCI two-stage ignition using multiple injection of synthetic fuels. In *Proceedings of ICEF2005, 2005 Fall Technical Conference of the ASME Internal Combustion Engine Division, September 2005, Ottawa, ON Canada*. ASME, 2005. ICEF2005-1282.

[4] C. J. Mueller, G. C. Martin, T. E. Briggs, and K. P. Duffy. An experimental investigation of in-cylinder processes under dual-injection conditions in a DI Diesel engine. SAE Paper No. 2004-01-1843, 2004.

[5] S. Pöttker, P. Eckert, T. Delebinski, C. Baumgarten, K. Oehlert, G. P. Merker, U. Wagner, and U. Spicher. Investigations of HCCI combustion using multi-stage direct-injection with synthetic fuels. SAE Paper No. 2004-01-2946, 2004.

[6] H. Ogawa, N. Miyamoto, A. Sakai, and K. Akao. Combustion in a two-stage injection PCCI engine with lower-distillation-temperature fuels. SAE Paper No. 2004-01-1914, 2004.

[7] R. Hasegawa and H. Yanagihara. HCCI combustion in DI diesel engine. SAE Paper No. 2003-01-0745, 2003.

[8] K. Yoshizawa, A. Teraji, H. Miyakubo, K. Yamaguchi, and T. Urushihara. Study of high load operation limit expansion for gasoline compression ignition engines. In *Proceedings of ICES2003, 2003 Spring Technical Conference of the ASME Internal Combustion Engine Division, May 2003, Salzburg, Austria*. ASME, 2003. ICES2003-543.

[9] Z. Wang, J.-X. Wang, S.-J. Shuai, and Q.-J. Ma. Effects of spark ignition and stratified charge on gasoline HCCI combustion with direct injection. SAE Paper No. 2005-01-0137, 2005.

[10] S. Yamamoto, T. Satou, and M. Ikuta. Feasibility study of two-stage hybrid combustion in gasoline direct injection engines. SAE Paper No. 2002-01-0113, 2002.

[11] T. Urushihara, K. Hiraya, A. Kakuhou, and T. Itoh. Expansion of HCCI operating region by the combination of direct fuel injection, negative valve overlap and internal fuel reformation. SAE Paper No. 2003-01-0749, 2003.

[12] M. Canakci, E. Hruby, and R. D. Reitz. Assessing double injection and intake air temperature effects on gasoline HCCI engine performance and emissions using fully automated experiments and micro-genetic algorithms. In *Proceedings of ICES2002, 2002 Spring Technical Conference of the ASME Internal Combustion Engine Division, April 2002, Rockford, Illinois USA*. ASME, 2002. ICES2002-459.

[13] K. Narayanaswamy and C. J. Rutland. Cycle simulation Diesel HCCI modeling studies and control. SAE Paper No. 2004-01-2997, 2004.

[14] H. Su, A. Vikhansky, S. Mosbach, M. Kraft, A. Bhave, F. Mauss, and K.-O. Kim. A new computational model for simulating direct injection HCCI engines. Technical Report 31, Cambridge Centre for Computational Chemical Engineering Preprint-Series, 2005. (submitted for publication).

[15] R. Jhavar and C. J. Rutland. Effects of mixing on early injection Diesel combustion. SAE Paper No. 2005-01-0154, 2005.

[16] S.-C. Kong, A. Patel, Q. Yin, and R. D. Reitz. Numerical modelling of Diesel engine combustion and emissions under HCCI-like conditions with high EGR levels. SAE Paper No. 2003-01-1087, 2003.

[17] L. Cao, H. Zhao, X. Jiang, and N. Kalian. Numerical study of effects of fuel injection timings on CAI/HCCI combustion in a four-stroke GDI engine. SAE Paper No. 2005-01-0144, 2005.

[18] Y. Sun, S.-J. Shuai, J.-X. Wang, and Y.-J. Wang. Numerical simulation of mixture formation and combustion of gasoline engines with multi-stage direct injection compression ignition (DICI). SAE Paper No. 2003-01-1091, 2003.

[19] S-C. Kong, Y. Ra, and R. D. Reitz. Performance of multi-dimensional models for simulating Diesel premixed charge compression ignition engine combustion using low- and high-pressure injectors. *Int. J. Engine Res.*, 6(5):475–486, 2005.

[20] W. Su, X. Zhang, T. Lin, Y. Pei, and H. Zhao. Study of pulse spray, heat release, emissions and efficiencies in a compound Diesel HCCI combustion engine. In *Proceedings of ICEF2004, 2004 Fall Technical Conference of the ASME Internal Combustion Engine Division, October 2004, Long Beach, California USA*. ASME, 2004. ICEF2004-927.

[21] A. Bhave, M. Kraft, F. Mauss, A. Oakley, and H. Zhao. Evaluating the EGR-AFR operating range of a HCCI engine. SAE Paper No. 2005-01-0161, 2005.

[22] S. B. Pope. PDF methods for turbulent reactive flows. *Prog. Energy Combust. Sci.*, 11:119–192, 1985.

[23] S. Subramaniam and S. B. Pope. A mixing model for turbulent reactive flows based on Euclidean minimum spanning trees. *Combust. Flame*, 115:487–514, 1998.

[24] H. Hiroyasu, T. Kadota, and M. Arai. Development and use of a spray combustion modeling to predict Diesel engine efficiency and pollutant emissions (part 1 combustion modeling). *Bulletin of the JSME*, 26(214):569–575, 1983.

[25] J. B. Heywood. *Internal Combustion Engine Fundamentals*. McGraw-Hill, New York, 1988.

[26] T. Jaine, A. Benkenida, P. Menegazzi, and P. Higelin. Zero dimensional computation of Diesel spray – comparison with experiments and 3D model. 6th International Conference on Engines for Automobile, Capri, Italy, 2003.

[27] C. T. Crowe, M. Sommerfeld, and Y. Tsuji. *Multiphase Flows with Droplets and Particles*. CRC Press LLC, 1997.

[28] M. Takagi and Y. Moriyoshi. Numerical simulations of spray formation process in high and low ambient pressures using a swirl-type injector. In *The Fifth International Symposium on Diagnostics and Modeling of Combustion in Internal Combustion Engines (COMODIA 2001), July 1-4, 2001, Nagoya*, 2002.